International Journal of Nanomedicine

Dovepress
open access to scientific and medical research

Open Access Full Text Article

ORIGINAL RESEARCH

Microenvironmental Enzyme-Responsive Methotrexate Modified Quercetin Micelles for the Treatment of Rheumatoid Arthritis

Xiuying Li[1], Xin Wang[1], Xiuwu Qu[1], Ningning Shi[1], Qinqing Li[1], Zhifang Yan[1], Yandong Li[2], Yingli Wang[3]

[1]Shanxi Key Laboratory of Innovative Drug for the Treatment of Serious Diseases Basing on the Chronic Inflammation, Shanxi University of Chinese Medicine, Jinzhong, People's Republic of China; [2]Xi'an International Medical Center Hospital, Xi'an, People's Republic of China; [3]Shanxi Modern Traditional Chinese Medicine Engineering Laboratory, Shanxi University of Chinese Medicine, Jinzhong, People's Republic of China

Correspondence: Yandong Li; Yingli Wang, Email liyandongzhongnan@163.com; wyl@sxtcm.edu.cn

Purpose: Rheumatoid arthritis (RA) is a chronic systemic autoimmune disease involving synovial inflammation and joint destruction. Although therapeutic drugs for RA have some efficacy, they usually cause severe side effects and are expensive. RA is characterized by synovial hyperplasia, intra-articular hypoxia, upregulated expression of matrix metalloproteinases, and excessive accumulation of reactive oxygen species. The adverse microenvironment further aggravates activated macrophage infiltration. Therefore, controlling the microenvironment of diseased tissues and targeting the activated macrophages have become new therapeutic targets in RA patients.

Methods: Here, microenvironment-targeting micelles (PVGLIG-MTX-Que-Ms) were synthesized using the thin film hydration method. In the inflammatory microenvironment, PVGLIG was cleaved by the highly expressed MMP-2, PEG_{5000} was eliminated, MTX was exposed, macrophage activation was targeted, and Que enrichment was enhanced. The cytotoxicity, targeting, antioxidant, and anti-inflammatory properties of drug-loaded micelles were tested in vitro. The drug-loaded micelles were used to treat CIA rats. In vivo targeting, expression of serum inflammatory factors, immunohistochemistry of the articular cartilage, and changes in immunofluorescence staining were observed.

Results: The developed micelles had a particle size of (89.62 ±1.33) nm and a zeta potential of (−4.9 ±0.53) mV. The IC_{50} value of PVGLIG-MTX-Que-Ms (185.90 ±6.98) μmol/L was significantly lower than that of free Que (141.10 ±6.39) μmol/L. The synthesized micelles exhibited slow-release properties, low cytotoxicity, strong targeting abilities, and significant anti-inflammatory effects in vitro. In vivo, the drug-loaded micelles accumulated at the joint site for a long time. PVGLIG-MTX-Que-Ms significantly reduced joint swelling, improved bone destruction, and decreased the expression of serum inflammatory factors in CIA rats.

Conclusion: The smart-targeting micelles PVGLIG-MTX-Que-Ms with strong targeting, anti-inflammatory, cartilage-protective, and other multiple positive effects are a promising new tool for RA treatment.

Keywords: matrix metalloproteinases, quercetin, macrophages, methotrexate, anti-inflammatory

Introduction

Rheumatoid arthritis (RA) is a chronic multisystem autoimmune disease that usually destroys joints and associated blood vessels symmetrically, which then affects metabolism and bones and triggers systemic complications.[1] RA is a highly prevalent disease, affecting approximately 2% of the global human population, with 70% of RA patients being women. Chronic inflammation-induced cardiovascular disease (CVD) remarkably increases RA-related mortality.[2] RA involves substantial medical expenses and causes a decline in physical function and quality of life, thereby placing a heavy burden on patients and their families.[3] RA is among the most important diseases jeopardizing human health, and its etiology remains unclear.[4]

Macrophages play a key role in RA-associated inflammation.[5] A large number of activated and aggregated macrophages in the synovial fluid and tissues can produce proinflammatory cytokines, chemokines, ROS, and matrix metalloproteinases

Received: 28 December 2023
Accepted: 25 March 2024
Published: 6 April 2024

(MMP). These factors promote and maintain inflammation, participate in RA vasculature proliferation, erode the articular surface, and exacerbate disease progression.[6,7] Therefore, targeting macrophage activation, reducing the expression of inflammation-related factors, and lowering the level of reactive oxygen species (ROS) in the microenvironment of diseased tissues are crucial for safe and effective RA treatment.[8]

Quercetin (Que), is a natural flavonoid and an active ingredient with anti-inflammatory, antioxidant, analgesic, and other beneficial effects and biological activities.[9,10] Preclinical or clinical studies have found Que effective in RA treatment by significantly reducing the levels of inflammatory cytokines and mediators and oxidative stress, with a strong therapeutic potential.[11,12] However, its poor solubility, poor gastrointestinal retention, low bioavailability, easy oxidation ability, and other defects markedly limit the efficacy of Que.[13]

A nanoparticle-targeted drug delivery system is associated with the advantages of low dose, low toxicity, and low side effects, and can selectively enrich the drug to the disease site. In RA, the synovial microenvironment is cytokine- and metabolite-rich, which results in a low pH environment, a hypoxic microenvironment, and MMP overexpression.[14,15] Designing an RA pathology-based delivery vehicle that responds in the inflammatory microenvironment and controls drug release may be a promising therapeutic strategy.

We here synthesized RA microenvironment-responsive micelles by using the upregulated MMP-2 enzyme in the RA microenvironment as a response condition. An MMP-responsive peptide (PVGLIG) was employed as a linker for conferring premedication to the polymers. Hydrophilic long-chain PEG_{5000} served as a hydration layer to prolong the somatic circulation time and enhance stability. To improve drug targeting, methotrexate (MTX) exhibiting a high affinity for folate receptor-β (FR-β), which is highly expressed on the surface of activated macrophages, was modified on the surface of Que-containing micelles.[16,17] We investigated the effects of targeted modulation of non-cytotoxicity of drug-loaded micelles on RA lesions through in vivo and in vitro experiments and evaluated their treatment effectiveness.

Materials and Methods

Materials, Cells and Animals

Que and Soluplus were obtained from Pufei De Biotech Co., Ltd (Chengdu, China) and Basf New Materials Co., Ltd. (Shanghai, China), respectively. $DSPEPEG_{2000}$-PVGLIG-PEG_{5000} and DSPE-PEG_{2000}-Methotrexate ($DSPEPEG_{2000}$-MTX) were synthesized by Ruixi Biological Technology Co., Ltd (Xi'an, China). Chicken type II collagen, complete Freund adjuvant, and incomplete Freund adjuvant were supplied by Chondrex, Inc. (Redmond, WA, USA). Lipopolysaccharide (LPS), TPGS1000, and 1.1-dioctadecyl-3,3,3,3-tetramethylindotricarbocyanine iodide (DiR) were provided by Meilun Co., Ltd (Dalian, China). ELISA kits and human active MMP2 proteins were purchased from Solarbio Co., Ltd (Beijing, China) and EMD Biosciences (La Jolla, CA, USA), respectively. All other reagents used were of analytical grade.

RAW264.7 cells were obtained from the Institute of Basic Medical Science, Chinese Academy of Medical Science (Beijing, China). The cells were cultured in DMEM supplemented with 10% fetal bovine serum and 1% penicillin-streptomycin solution (100 U/mL penicillin and 100 μg/mL streptomycin) in a humidified atmosphere of air and CO_2 (95% and 5%) at 37°C. Specific pathogen-free female Sprague-Dawley rats (140–160 g) were bought from Changsheng Biotechnology Co., Ltd (Liaoning, China). All animals were kept at a constant temperature of 22°C–24°C and a humidity of 55%–60%. All experimental procedures were strictly conducted according to the Guidelines for Ethical Review of Laboratory Animal Welfare in China (GB/T3589-2018). The study protocol was approved by the Animal Research Ethics Committee of Shanxi University of Chinese Medicine (Approval No. AWE202302038).

Micelle Preparation

PVGLIG-MTX-Que-Ms were synthesized using the thin-film hydration method. Soluplus, TPGS1000, DSPE-PEG_{2000}-PVGLIG-PEG_{5000}, DSPE-PEG_{2000}-MTX, and Que were mixed and dissolved in methanol in a round-bottomed flask and spun into a thin film at 40°C. The product was hydrated with 5 mL phosphate buffer (PBS, pH = 7.4) and passed twice through a 0.22-μm microporous filter membrane to obtain PVGLIG-MTX-Que-Ms. Que-Ms and MTX-Que-Ms were synthesized similarly. Various micelles were synthesized by replacing Que with coumarin (Cou) or DiR.

Characterization of Micelles

The CMC of the synthesized micelles was determined using the pyrene fluorescence probe method.[18] A dynamic light scatterometer was used to determine the micelle size, polydispersity index (PDI), and zeta potential (Litesiezr 500; Anton Paar Instruments Ltd., Graz, Austria). Phosphotungstic acid negative staining was performed to stain the micelles and observe their morphology through transmission electron microscopy (TEM, JEM-1200EX; JEOL, Tokyo, Japan). The Sephadex G50 column was used to remove the unencapsulated Que, and high-performance liquid chromatography (D1100, Dalian Elite) was performed to determine the encapsulation efficiency (EE). Que was assayed on an UltimateXB-C18 column (4.6 mm×250 mm, 5 μm) with a flow rate of 1 mL/min. The mobile phase was methanol-0.05% phosphoric acid (65:35). The detection wavelength, column temperature, and liquid phase injection volume were 360 nm, 25°C, and 20 μL, respectively. The EE was calculated as follows: $EE\% = (E_1/E_2) \times 100\%$, where E_1 and E_2 are the mass of Que-loaded micelles and the total mass, respectively.

To analyze the micellar release rate in vitro, the micelles were dialyzed using the PBS buffer solution containing 10% FBS. First, 1 mL PVGLIG-MTX-Que-Ms was added to the dialysis bag and shaken slowly at 37°C. To simulate the arthritic synovial microenvironment, 1.5 μg/mL MMP2 enzyme was added to the release medium. Sucking an appropriate amount of buffer, the Que content of the samples was determined at 6, 12, 24, 48, and 72 h. To evaluate micelle stability, the samples were stored at 4°C for 7 days, and the particle size, PDI, and EE% of the micelles were determined.

Hemolysis experiments were conducted to evaluate the safety of the use of micelle injection. Whole blood was collected from the rats. Red blood cells were separated following centrifugation and resuspended in normal saline to a 2% concentration (w/v). Then, 1.5 mL of the red blood cells was added to 100 μM PVGLIG-MTX-Que-Ms and incubated at 37°C for 3 h. For this analysis, 1.5 mL of both normal saline and water was used as negative and positive controls, respectively. The absorbance value of the supernatant at 540 nm was measured after 1 mL of the suspension was centrifuged. Hemolysis percentage = $[(A_a-A_0)/(A_b-A_0)] \times 100\%$, where A_0, A_b, and A_a denote negative control, positive control, and PVGLIG MTX-Que-Ms absorbance, respectively.

RAW264.7 Cell Viability

The sulforhodamine B (SRB) assay was performed to detect the effect of free drugs and various groups of micelles on cell viability. RAW264.7 cells (5×10^3 cells/well) were inoculated in 96-well plates and treated with different micelle groups after incubation for 12 h. After the treated cells were incubated for 48 h, the medium was discarded. The cells were then incubated with 10% trichloroacetic acid for 1 h, washed, stained with SRB for 20 min, and washed with 1% acetic acid solution. Tris buffer was added, and absorbance was measured at 540 nm by using an enzyme meter (HBS-1096A, DeTie, Nanjing, China). Cell survival was calculated as follows: $S\% = (S_1/S_2) \times 100\%$, S_1 and S_2 represent the absorbance values of the treated and control cells, respectively. The 50% inhibitory concentration (IC_{50}) was calculated using GraphPad Prism 6.0 software (La Jolla, CA, USA).

Calcein AM/PI Staining

RAW264.7 cells (3×10^5 cells/well) were cultured in 6-well plates. After 12 h of adherence culture, the cells were treated with different micelle groups (Que, 150μM). Following 24 h of incubation, the medium was discarded, the cells were washed with PBS, and an appropriate amount of Calcein AM/PI working solution was added. The cells were incubated for 30 min at 37°C without being exposed to light. The stained cells were imaged under a fluorescence microscope (Nikon Ti–S, Tokyo, Japan).

Cellular Uptake

The targeting effects of different micelles on RAW264.7 cells and LPS-induced RAW264.7 cells were observed through fluorescence microscopy. The RAW264.7 cells (1×10^5 cells/well) were inoculated in 48-well plates. Once the cells had adhered to the wall, LPS (100 ng/mL) was added to induce them.[19] Following 12 h of incubation, the original medium was replaced with the medium containing different micelle groups (Blank-Ms, Cou-Ms, MTX-Cou-Ms, and PVGLIG-MTX-Cou-Ms). The enzyme-responsive drug-carrying micelles were divided into two groups. One

group was pre-incubated overnight with MMP2.[20,21] After 2 h of incubation, the cells were fixed in 4% paraformaldehyde solution and stained with DAPI for 10 min while being protected from light. The fluorescence intensity distribution of the cells was observed using the fluorescence microscope. Flow cytometry (BD Biosciences, Franklin Lakes, NJ, USA) was performed to further quantify the uptake of different micelles by cells. The RAW264.7 cells were also treated as mentioned above, and the cells' average fluorescence intensity was determined through flow cytometry.

In vitro Pro-Inflammatory Factor Assay

The expression of proinflammatory factors in LPS-induced RAW264.7 cells treated with each micelle group was determined. The RAW264.7 cells (1.5×10^5 cells/well were inoculated in 6-well plates. Once the cells had adhered to the wall, LPS was added to induce the cells. After 6 h, the cells were treated with different micelle groups (Blank-Ms, Que-Ms, MTX-Que-Ms, and PVGLIG-MTX-Que-Ms; Que, 150μM). The supernatant was collected after 24 h of incubation. TNF-α, IL-6, and IL-17 expression levels were detected using the ELISA kit.

ROS Measurement

The DCFH-DA probe was used to detect intracellular ROS expression. RAW264.7 cells (3×10^5 cells/well) were cultured in 48-well plates. Each cell group, including the blank group, was induced by adding LPS. After 6 h, different micelle groups (Blank-Ms, Que-Ms, MTX-Que-Ms, and PVGLIG-MTX-Que-Ms; Que, 150μM) were added. After 24 h of incubation, the medium was discarded. The probe diluted with serum-free medium was added to the cells and incubated. The probe-treated cells were statistically observed under the fluorescence microscope.

CIA Rats Model Establishment and Drug Administration

CFA, IFA, and C type II collagen (2 mg/mL) were homogeneously emulsified in equal volumes under sterile conditions in an ice bath at 4°C. On days 0 and 7, small amounts of the suspension emulsion were intradermally injected into the rats at multiple locations, starting from the root of the rat's tail, to establish CIA rats.[22] The CIA rats were injected intravenously with the therapeutic preparations of each group (Que: 10 mg/kg), and saline was administered to the control group. The arthrographic index of the rats in each group was recorded. At the same time, the body weight of the rats was measured every 3 days for a total of 27 days. Photographs of the degree of swelling in the hind paws of the rats in each group were taken on the 27th day.

In vivo Imaging of CIA Rats

Joint targeting was evaluated through in vivo fluorescence imaging. DiR, a fluorescent probe, was loaded into individual micelles instead of Que to form DiR-Ms. The CIA rats were intravenously injected with DiR-Ms, MTX-DiR-Ms, PVGLIG-MTX-DiR-Ms, and free DiR (DiR, 400 μg/kg; n=3). Photographs were taken at 4, 8, 12, 24, 36, 48, and 72 h by using an in vivo fluorescence imaging system (IVScope 8200, Clinx, China).

Serum Inflammatory Factor Measurement

At the end of the experiment on the 27th day, blood was collected from the orbits of the rats and centrifuged at 3000 r/min for 5 min at 4°C. The supernatant was collected and tested for the relevant indices by using the same procedure as given in subsection 2.7.

Histological Analysis

After the last administration, the rats were euthanized, and their hearts, livers, spleens, lungs, kidneys, knee joints, and ankle joints were removed and collected. The tissue samples were fixed in 4% paraformaldehyde, embedded in paraffin, sectioned, and stained with hematoxylin-eosin. The joints were stained with Safranin-O and analyzed immunohistochemically. CD44 and CD68 expression in the cartilage was detected using the immunofluorescence method. Pathological changes in various tissues and organs of rats were observed under the light microscope.

Statistical Analysis

All results were expressed as mean ± standard deviation and statistically analyzed using GraphPad Prism 6.0. Intergroup ratios were assessed using a one-way analysis of variance. Post hoc multiple comparisons were performed using the Student–Newman–Coors test. A difference of $P < 0.05$ was considered statistically significant.

Results

Characterization of Micelles

Figure 1A–F presents the characteristics of the drug-carrying micelles. The critical micelle concentration of PVGLIG-MTX-Que-Ms is shown in Figure 1A, which was 0.0146 mg/mL. This indicated that the lower CMC value ensures that the diluted micelles are stable in vivo and facilitate circulation. TEM images (Figure 1B) revealed that the prepared micelles were spherical with smooth surfaces and had a uniform distribution. The hemolysis assay (Figure 1C) unveiled that the drug-loaded micelles exhibited no significant hemolytic activity in the 0.1–1 mg/mL concentration range. The average particle size of PVGLIG-MTX-Que-Ms was (89.62 ±1.33) nm (Figure 1D) and the zeta potential was (−4.9 ±0.53) mV (Figure 1E). Figure 1F–I presents the EE, particle size, zeta potential, and PDI of different micelles. The encapsulation rates of MTX-Que-Ms and PVGLIG-MTX-Que-Ms were (91.88 ±4.42)% and (90.80 ±2.84)%, respectively, and the particle size of all micelle groups was approximately 90 nm. After target molecules and enzyme-responsive target molecules were added, the zeta potential of the micelles changed and approached −5 mV. We monitored the in vitro release behavior of Que-loaded micelles kinetically in a simulated microenvironment of PBS solution. Figure 1J presents the release characteristics. Within 12 h, the release rates of both were similar and within 72 h, the release rate of PVGLIG-MTX-Que-Ms was (69.26 ±3.13)%, which is a relatively fast release rate. While in the MMP2 enzyme-containing environment, the release rate of PVGLIG-MTX-Que-Ms was (52.31 ±1.65)%, which was relatively slow. After 7 days of storage at 4°C (Figure 1K and L), the PDI value of the drug-loaded micelles increased slightly, the particle size exhibited no significant change, the finished product exhibited no precipitation, and the encapsulation rate decreased slightly but was >80%. The variations were all within the appropriate range.

Cell Viability and Calcein-AM/PI Staining Assays

The cytotoxicity of different free Que concentrations and each micelle group on RAW264.7 cells was investigated using the SRB method (Figure 2A and B). The IC_{50} values of Que-Ms, MTX-Que-Ms, PVGLIG-MTX-Que-Ms, and PVGLIG-MTX-Que-Ms in the MMP-2 enzyme-rich environment and free Que were (185.90 ±6.98) μmol/L and (165.17 ±6.11) μmol/L, (175.70 ±11.09) μmol/L, (175.01 ±5.53) μmol/L, and (141.10 ±6.39) μmol/L, respectively. After 48 h of incubation, at 150 μmol/L Que, the cell survival rate was lower in the free group, whereas that in each preparation group was >50%. The cytotoxicity of PVGLIG-MTX-Que-Ms was lower than that of the same concentration of free Que. Figure 2C presents the results of Calcein-AM/PI staining. In staining, that is, dead cells were stained red, whereas living cells were stained green. In the free Que group, the number of dead cells and PI positivity were high. The number of dead cells in the PVGLIG-MTX-Que-Ms group was significantly lower than that in the free Que group, which indicated that Que cytotoxicity was significantly reduced after being introduced into micelles.

Cellular Uptake and Distribution

Cou has strong fluorescence and was used as a drug replacement fluorescent tracer. Figure 3A presents the results of cellular uptake observed through fluorescence microscopy. The RAW264.7 cells in each agent group exhibited similar uptake without significant difference (Figure 3B). The LPS-activated RAW264.7 cells, which exhibited stronger fluorescence. Cou-Ms exhibited a certain amount of drug uptake, whereas the fluorescence intensity was more intense and the uptake increased in the case of MTX-Cou-Ms. The fluorescence signal of PVGLIG-MTX-Cou-Ms was lower and similar to that of Cou-Ms. However, the fluorescence signal of PVGLIG-MTX-Cou-Ms significantly improved when the cells were incubated with the MMP2 enzyme-containing culture medium (Figure 3C). Uptake was further quantified through flow cytometry (Figure 3D and E). Activated macrophages exhibited higher drug uptake (Figure 3F). The

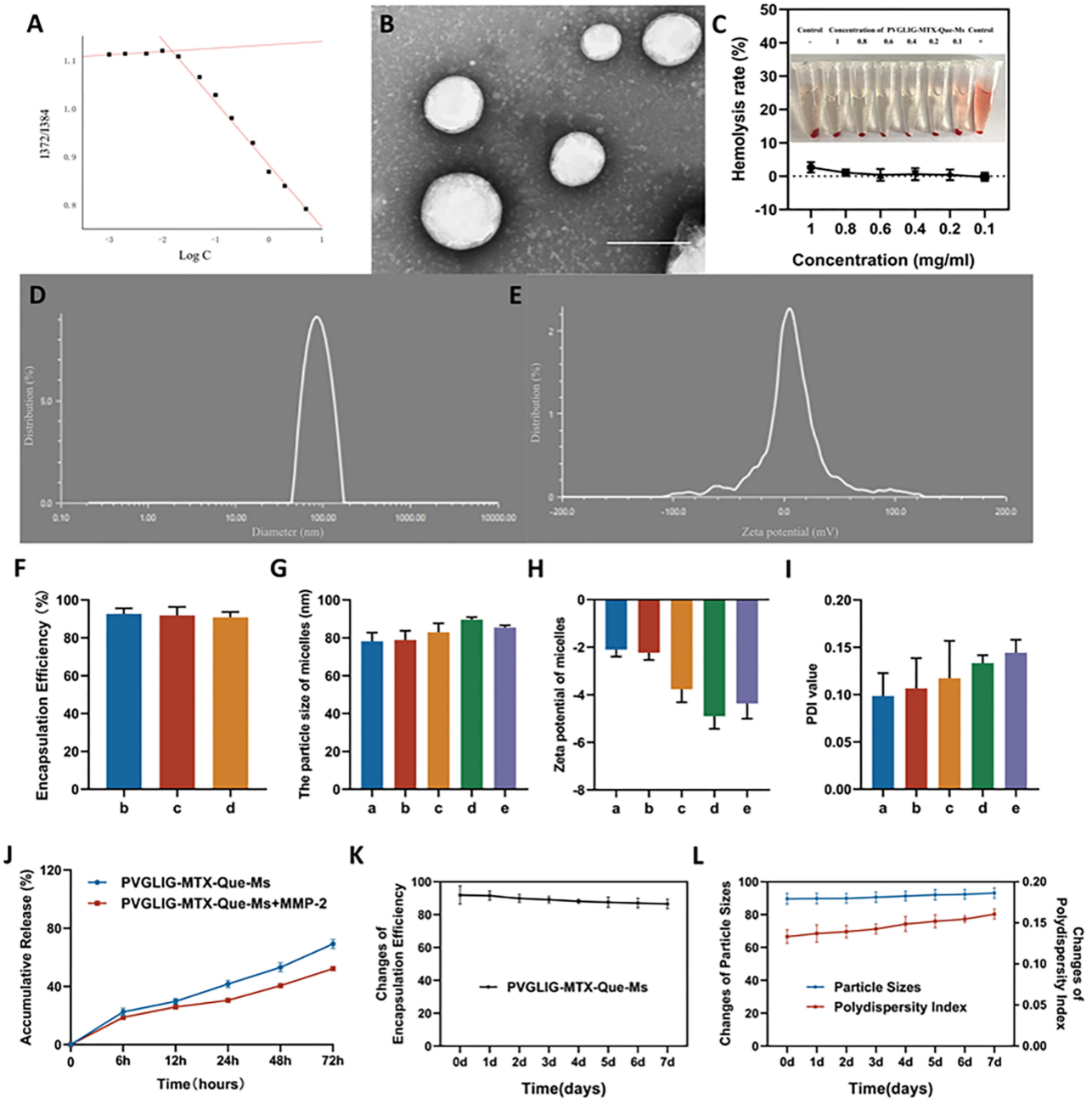

Figure 1 Characterization of PVGLIG-MTX-Que-Ms. (**A**) The variations in fluorescence intensity ratio (I372/I384) as a function of the concentration of PVGLIG-MTX-Que-Ms. (**B**) Transmission electron microscope (TEM) image of PVGLIG-MTX-Que-Ms. Scale bar, 100 nm. (**C**) Hemolysis of induction of PVGLIG-MTX-Que-Ms. (**D**) Particle size distribution of PVGLIG-MTX-Que-Ms. (**E**) Zeta potential distribution of PVGLIG-MTX-Que-Ms. (**F**) Encapsulation rate of micelles. (**G**) Quantitative analysis of particle size of micelles. (**H**) Quantitative analysis of zeta potential distribution of micelles. (**I**) Quantitative analysis of PDI value of micelles. (**J**) Release rate of quercetin from the varying formulations. (**K**) Change of encapsulation efficiency of PVGLIG-MTX-Que-Ms of 7 days. (**L**) Change of particle sizes and PDI value of PVGLIG-MTX-Que-Ms of 7 days. Data are presented as mean ± SD (n=3). a, Blank-Ms. b, Que-Ms. c, MTX-Que-Ms. d, PVGLIG-MTX-Que-Ms. e, PVGLIG-MTX-Que-Ms in MMP-2 enzyme-rich environment.

average FL1-H of the PVGLIG-MTX-Cou-Ms-treated cells was significantly higher than that of the Cou-Ms-treated cells in the presence of the MMP2 enzyme (Figure 3G), which was in agreement with the aforementioned observations.

Inflammatory Cytokines and ROS Generation Assays

TNF-α, IL-6, and IL-17 are proinflammatory cytokines with a key role in RA pathogenesis. The anti-inflammatory effects of drug-loaded micelles on activated macrophages were investigated (Figure 4A–C). After the cells were induced with

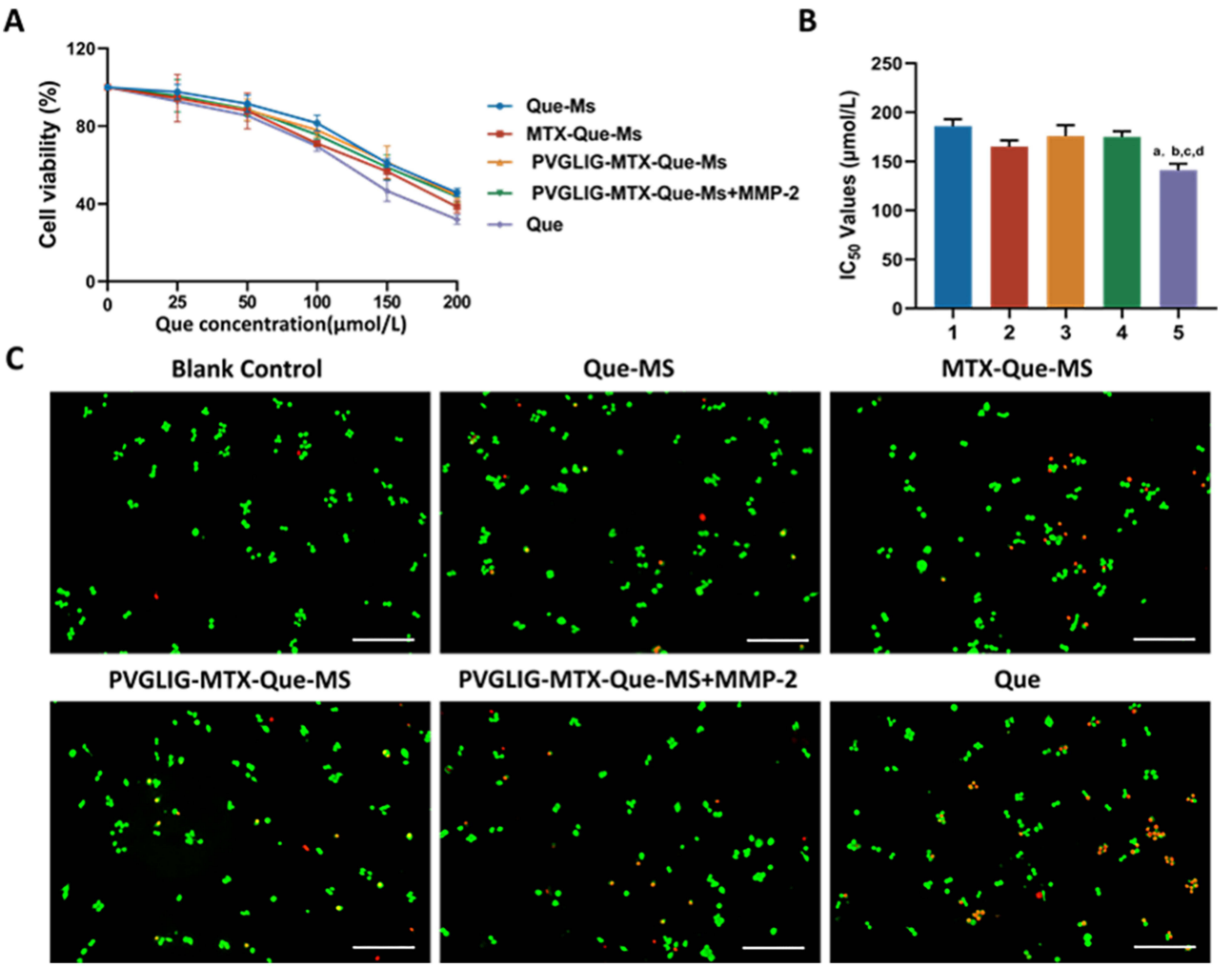

Figure 2 Cell viability and calcein-AM/PI staining assays on RAW264.7 cells after incubation with varying formulations. (**A**) The growth curves of free drugs and micelles of RAW264.7 cells at varying concentrations of Que. (**B**) Statistical analysis of IC_{50} values of varying formulations. 1, 2, 3, 4, vs Que. $P<0.05$. (**C**) Calcein-AM/PI staining assays after incubation with varying formulations. Data are presented as mean ± SD (n=3). 1, Que-Ms. 2, MTX-Que-Ms. 3, PVGLIG-MTX-Que-Ms. 4, PVGLIG-MTX-Que-Ms in MMP-2 enzyme-rich environment. 5, free Que.

LPS, the levels of the aforementioned three proinflammatory factors increased significantly in the cell supernatant, and the secretion of these proinflammatory factors was inhibited by all the preparation groups. Although the inhibitory effect of PVGLIG-MTX-Que-Ms was slightly weaker, the inhibitory effect significantly increased in an MMP2-rich environment, thus achieving an inhibitory effect similar to that of MTX-Que-Ms. ROS overproduction is closely related to RA onset and development. The DCFH-DA probe was used to detect intracellular ROS expression and analyze the results statistically (Figure 4D and E). Compared with the model group, drug-loaded micelles significantly inhibited intracellular ROS production, and PVGLIG-MTX-Que-Ms exerted better inhibitory effects in the MMP2 enzyme-enriched culture medium.

CIA Rat Imaging in vivo

Figure 5 presents the representative images of the hind limbs of the CIA rats after they were injected with each preparation through the tail vein. Almost no fluorescence signal indicating free DiR accumulation at the joints was noted. The fluorescence signals and durations of DiR-Ms and MTX-DiR-Ms were similar and concentrated in the joints, with stronger fluorescent signal values observed from 0 to 12 h, a significant decrease in the signal values after 24 h, and almost no fluorescent values observed at 72 h. PVGLIG-MTX-DiR-Ms-treated inflamed joints had the strongest

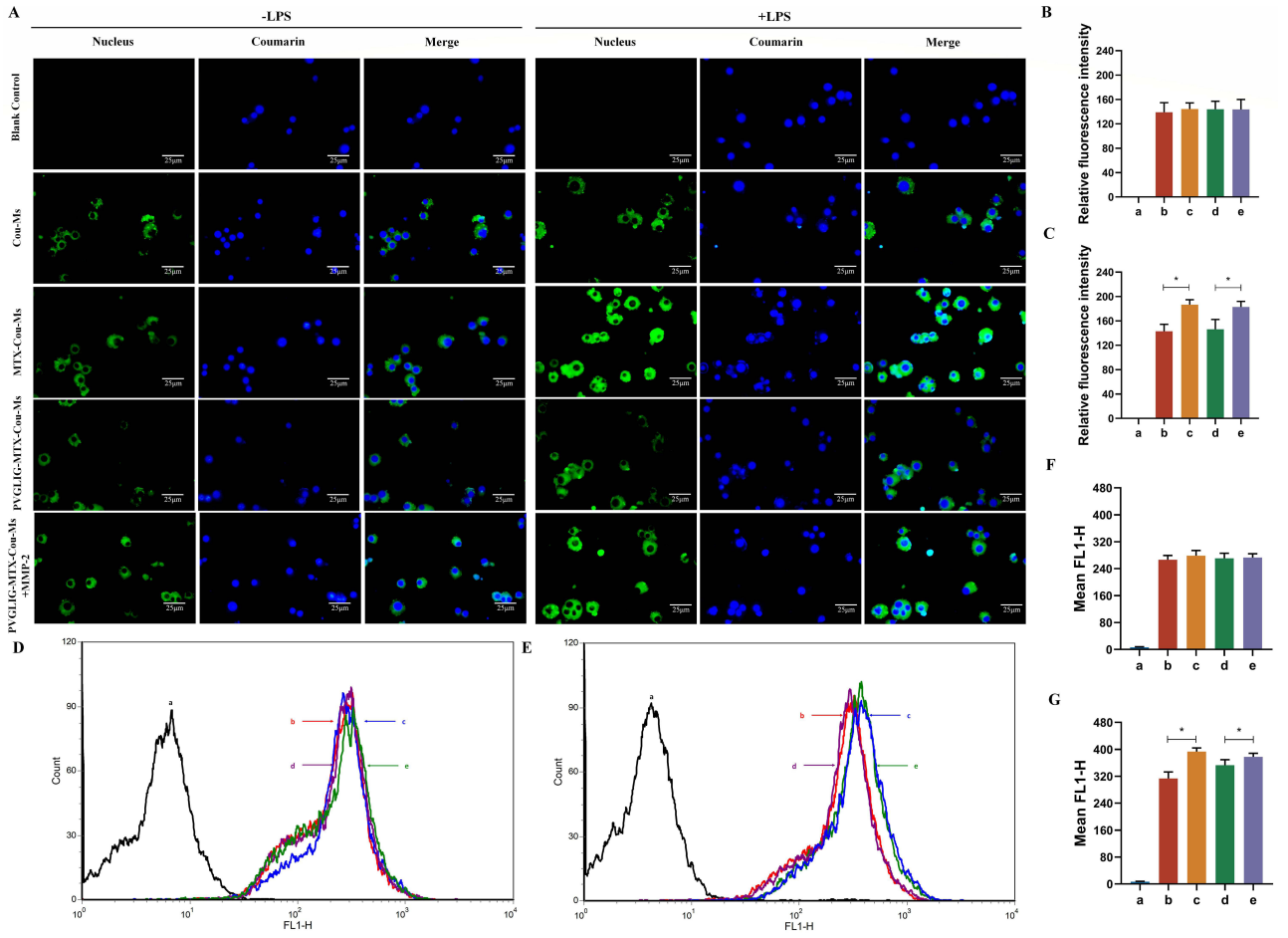

Figure 3 Cellular uptake and distribution after incubation with varying formulations. (**A**) Fluorescence microscopy images of RAW264.7 cells treated with or without LPS with different formulations. Scale bar, 25 μm (n=3). (**B** and **C**) Quantitative analysis of fluorescence intensity for different formulations. (**D** and **E**) The uptake of different formulations to cells treated without or with LPS. (**F** and **G**) Relative fluorescence intensity of varying formulations to cell. Data are presented as mean ± SD (n=3). * P < 0.05. a, Blank control. b, Cou-Ms. c, MTX-Cou-Ms. d, PVGLIG-MTX-Cou-Ms. e, PVGLIG-MTX-Cou-Ms in MMP-2 enzyme-rich environment.

fluorescence signal values and the longest duration values. A small amount of fluorescence accumulation was also observed in both joints at 72h.

CIA Rat Anti-Arthritic Efficacy

The anti-inflammatory effect of drug-loaded micelles on CIA rats was evaluated using four methods: hind limb photography, toe thickness measurement, joint scoring, and serum inflammatory factor analysis. The CIA rat model was successfully established. Figure 6A shows the representative pictures of the hind paws of rats in each group at the end of the experiment. Compared with the control group, the model and free Que groups exhibited obvious redness, swelling, and deformation of the toes. Following treatment with the drug-loaded micelles, the swelling improved in all the groups. The best effect was observed in the PVGLIG-MTX-Que-Ms treatment group, with no redness, swelling, or deformation of toes noted at the end of the treatment. Figure 6B presents the statistical results of toe thickness. After the 15th day, a significant difference was observed between the PVGLIG-MTX-Que-Ms-treated CIA rats and the model group rats. After the 27th day, toe thickness in the PVGLIG-MTX-Que-Ms-treated CIA rats reduced to (6.32 ±1.05) nm, which was basically the same as that in the control rats. Changes in joint scores are presented in Figure 6C. The joint scores of rats in all treatment groups exhibited a decreasing trend, with the PVGLIG-MTX-Que-Ms-treated rats exhibiting the best effect. Three inflammatory factors were analyzed in the serum of CIA rats (Figure 6D–F). Compared with the model group, drug-loaded micelles significantly inhibited

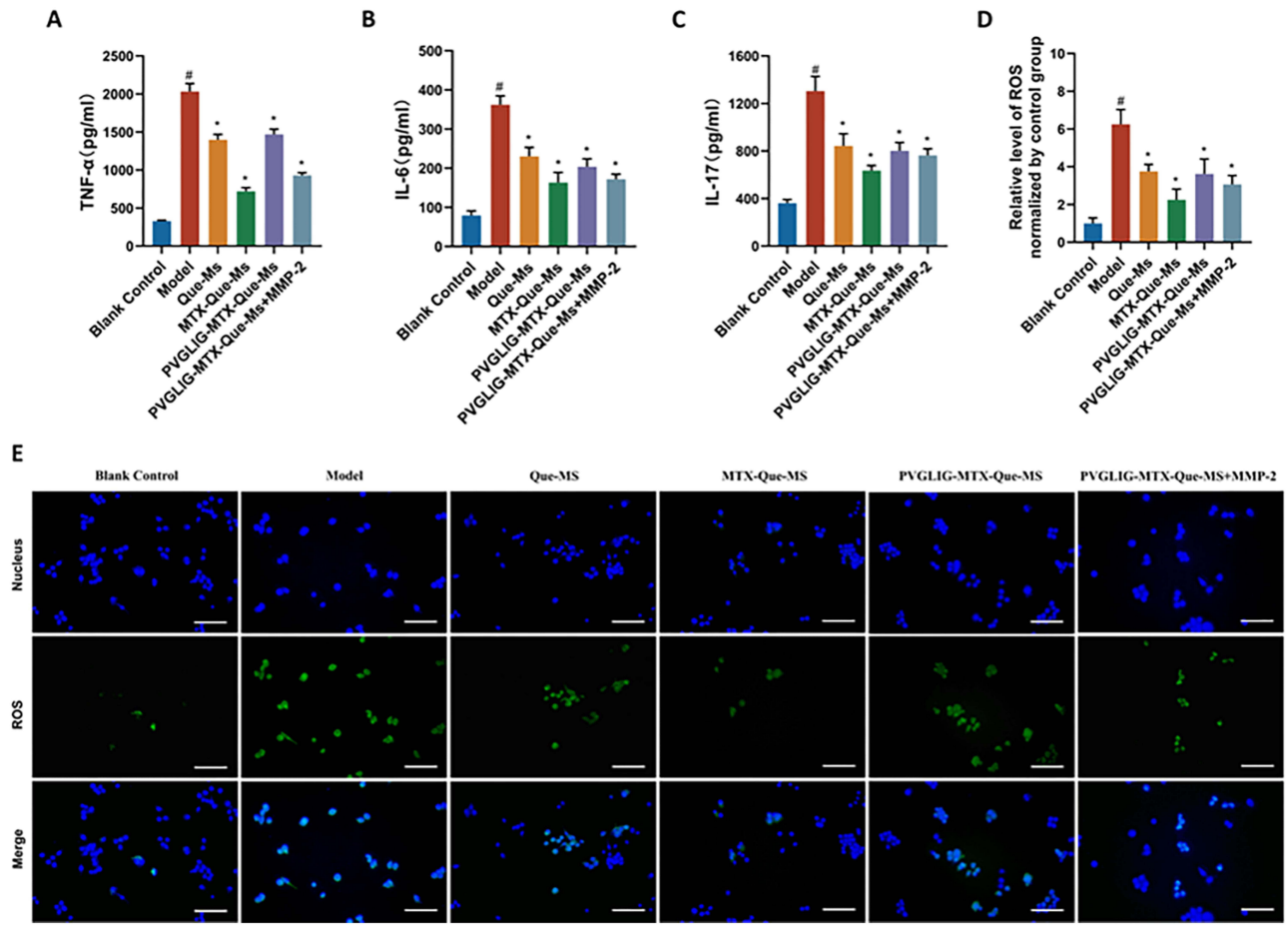

Figure 4 Effect on production of inflammatory cytokines and ROS generation assays of varying formulations on RAW264.7 cells. (**A-C**) TNF-α, IL-6, and IL-17 levels in the supernatant of RAW264.7 cells activated by LPS treated with varying formulations. Data are presented as mean ± SD (n=3). #, vs Blank Control; *, vs Model. P < 0.05. (**D**) Statistics of inhibitory effects of different dosage forms on ROS production in RAW264.7 cells. Data are presented as mean ± SD (n=3). #, vs Blank Control; *, vs Model. P < 0.05. (**E**) Inhibitory effects of formulations on ROS production in RAW264.7 cells. Scale bar, 50 μm. (n=3).

IL-17, IL-6, and TNF-α production. PVGLIG-MTX-Que-Ms decreased the production of these three factors most significantly.

Histology Analysis and Safety Evaluation in vivo

Knee and ankle joints were stained with HE and Safranin-O, respectively (Figure 7A–D). The joint surface of the model group was uneven, with synovial tissue hyperplasia. It had a rough border and unclear and disorganized arrangement. The cartilage surface was damaged, and the cells exhibited a disordered distribution, with bone missing. After the joints were treated with the drug-loaded micelles, cartilage degeneration was evidently suppressed. The degree of bone destruction was significantly reduced. The articular surface in the PVGLIG-MTX-Que-Ms treatment group was restored to become smooth, and the cartilage structure was close to normal. These findings indicated that the effect of PVGLIG-MTX-Que-Ms treatment was the most remarkable. Figure 7E and F presents the results of immunofluorescence staining of CD44 and CD68 in cartilage tissues. Compared with the control group, CD44 and CD68 were distributed in large quantities in the cartilage of the model group. Compared with the model group, CD44 and CD68 expression was significantly reduced in the cartilage of the PVGLIG-MTX-Que-Ms group. HE staining of the main rat organs in each group revealed no obvious histological damage or changes in these organs in each group after being treated with the drug-loaded micelles, which indicated that PVGLIG-MTX-Que-Ms has a good safety profile and no obvious systemic toxicity (Figure 8).

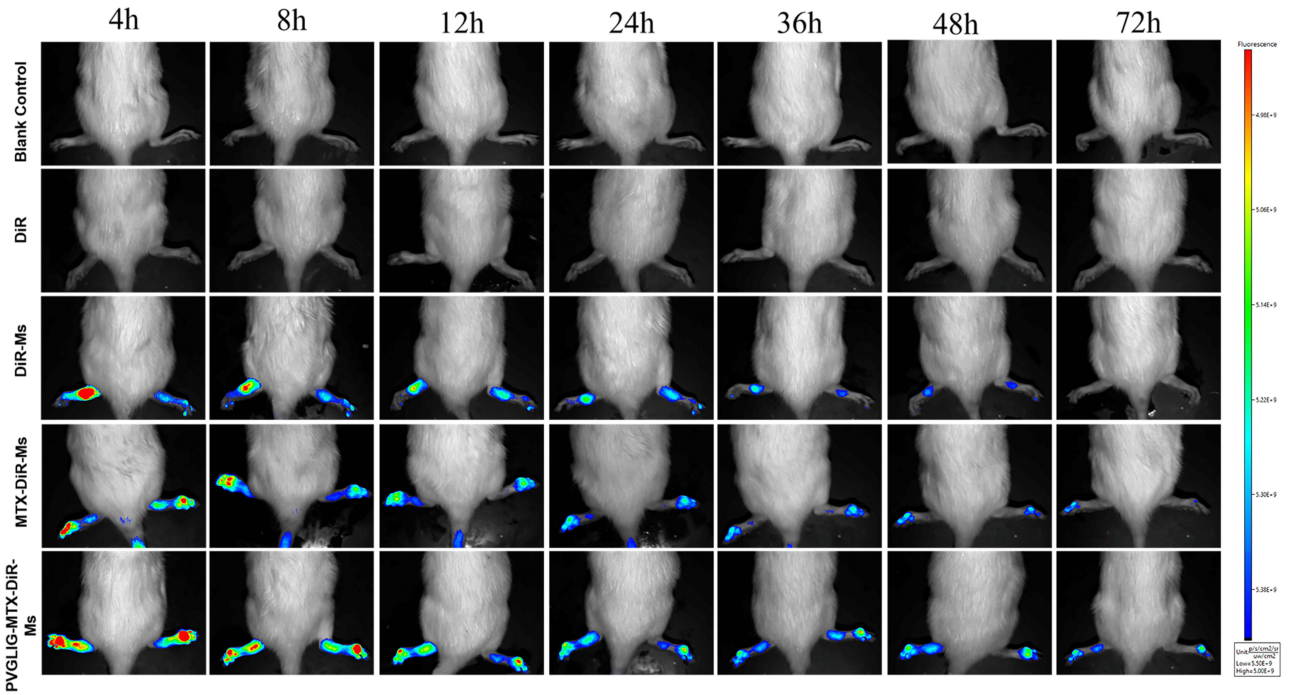

Figure 5 Real-time imaging observation of CIA rats after intravenous injection of different micelles.

Discussion

PVGLIG-MTX-Que-Ms were synthesized to explore their anti-inflammatory therapeutic potential in activated macrophages and the CIA arthritis rat model. The physicochemical properties of the micelles are among the crucial indices for evaluating micelles. The prepared drug-carrying micelles had smooth surfaces, were spherical, had narrow and uniform particle size distributions, showed negative electronegativity, and had an encapsulation rate of >90% in all the groups. PVGLIG is an MMP2 enzyme-specific reactive peptide used in RA microenvironment-targeted drug delivery systems.[23] In the presence of MMP2, PVGLIG on micelles is enzymatically cleaved and the particle size becomes smaller. Which gets aggregated at the inflammation site by the ELVIS effect.[24] To evaluate the hemocompatibility of the drug-carrying micelles, we conducted hemolysis experiments.[25] The groups in which different concentrations of drug-carrying micelles were used exhibited a pale yellow color, whereas the positive control group displayed a bright red color with an extremely high hemolysis rate. This indicated that the drug-loaded micelles exhibited good biocompatibility, and so could be intravenously administered within a certain range. Polyethylene glycolization helped the drug-loaded micelles to evade the clearance by the reticuloendothelial system. We simulated the RA microenvironment with high MMP2 enzyme expression in vitro to observe the drug release efficiency. Compared with the PBS control solution without the MMP2 enzyme, PVGLIG demonstrated a slow release after being hydrolyzed and destroyed by the MMP2 enzyme, thereby allowing the drug-carrying micelles to accumulate in the target tissues, delaying drug release, and prolonging the drug efficacy. PVGLIG-MTX-Que-Ms displayed good sensitivity to the MMP2 enzyme, which enabled it to target inflammatory joints for specific release. Changes in the particle size and PDI of the loaded micelles were within reasonable limits within 7 days at 4°C, which indicated good stability, probably because of the enhancement of retention time by DSPE-PEG_{2000}.[26]

Que has some toxicity, hence we conducted cytotoxicity experiments. The survival rate of the RAW264.7 cells depended on concentration. The cytotoxicity of the drug-loaded micelles was lower than that of free Que. When the MMP2 enzyme was present, the toxicity of PVGLIG-MTX-Que-Ms slightly changed. However, no significant difference was observed in the results in the absence of the MMP2 enzyme, This result combined with those of Calcein-AM/PI staining indicated that the micelles had good safety, which effectively reduced free Que

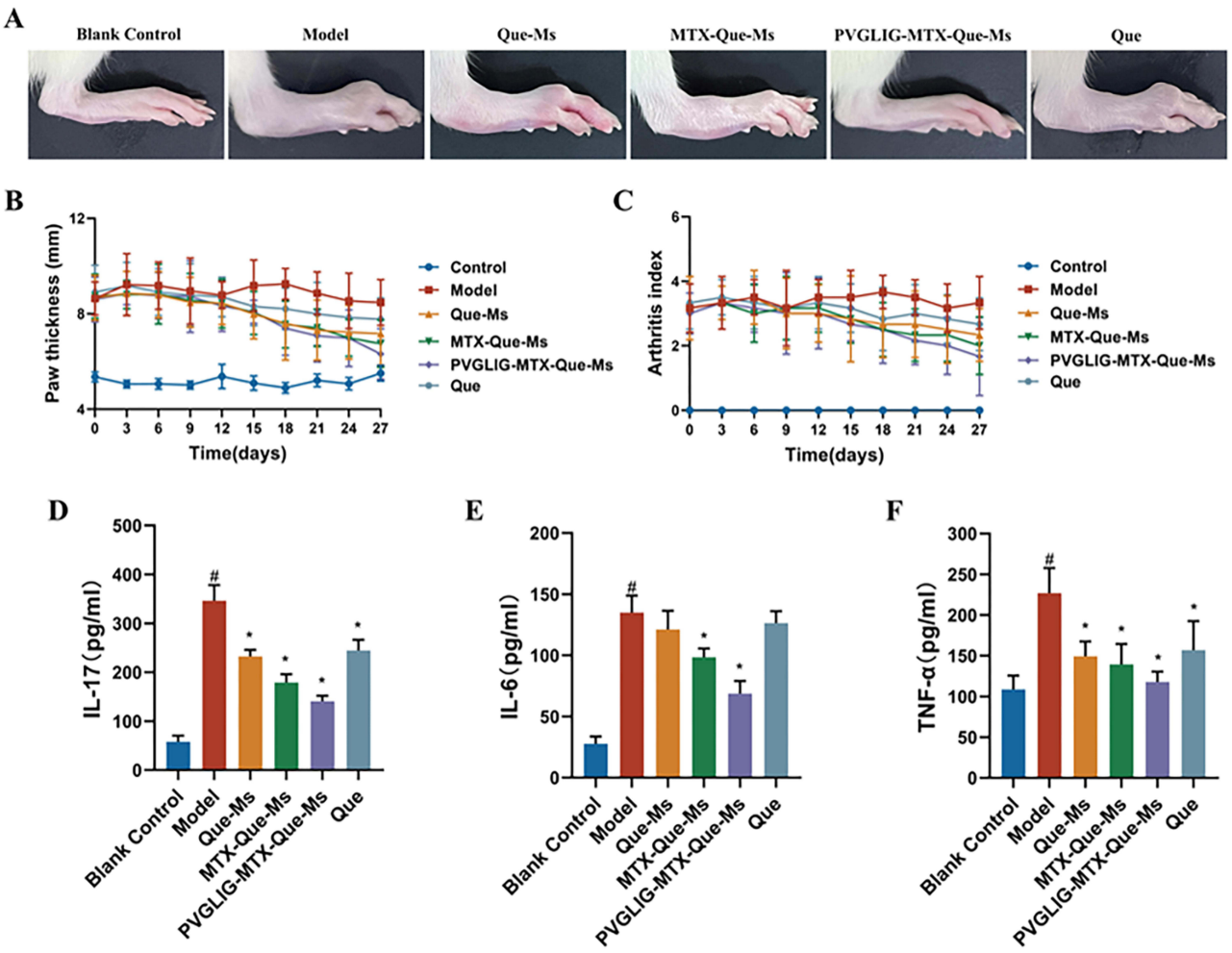

Figure 6 Anti-arthritic efficacy in CIA rats. (**A**) Representative photographs of hind paws at the end point of the experiment from each group. (**B**) Paw thickness of arthritic rats during the treatment of varying formulations. (**C**) Arthritis index score of arthritic rats during the treatment of varying formulations. (**D-F**) The levels of IL-17, IL-6, and TNF-α in the serum of CIA rats. #, vs Blank Control; *, vs Model. P < 0.05. Data are presented as the mean SD (n=6).

cytotoxicity and delayed drug release. The differences in the ability of the drug-loaded micelles to target activated and non-activated macrophages were assessed through fluorescence microscopy and flow cytometry. Considerably, the two methods produced consistent results. The drug-loaded micelles were efficiently taken up by the macrophages, with more uptake and stronger fluorescence exhibited by activated macrophages. When incubated with the MMP2 enzyme, PVGLIG-MTX-Que-Ms first reacted with the enzyme and was then degraded, which exposed the target molecule MTX. MTX was bound specifically to the activated macrophages and recovered to the same level as MTX-Que-Ms. Both qualitative and quantitative results indicated that the micelles effectively targeted activated macrophages to release drugs and that PVGLIG-MTX-Que-Ms cellular uptake was maximized in the RA microenvironment. In RA inflammation, activated macrophages secrete large amounts of proinflammatory cytokines and ROS, which induce inflammatory cell infiltration and destroy cartilage and bone tissues.[27,28] All the drug-loaded micelles in the present study reduced TNF-α, IL-6, IL-17, and ROS production and expression. PVGLIG-MTX-Que-Ms had some anti-inflammatory capacity. This capacity significantly increased after the MMP2 enzyme was added to the simulated RA microenvironment; this result was in agreement with those of the cellular uptake experiments.

Animal models can help in understanding disease development more easily and efficiently and investigating prevention and treatment measures. Histological and immunological changes in the CIA rat model are very similar to those in

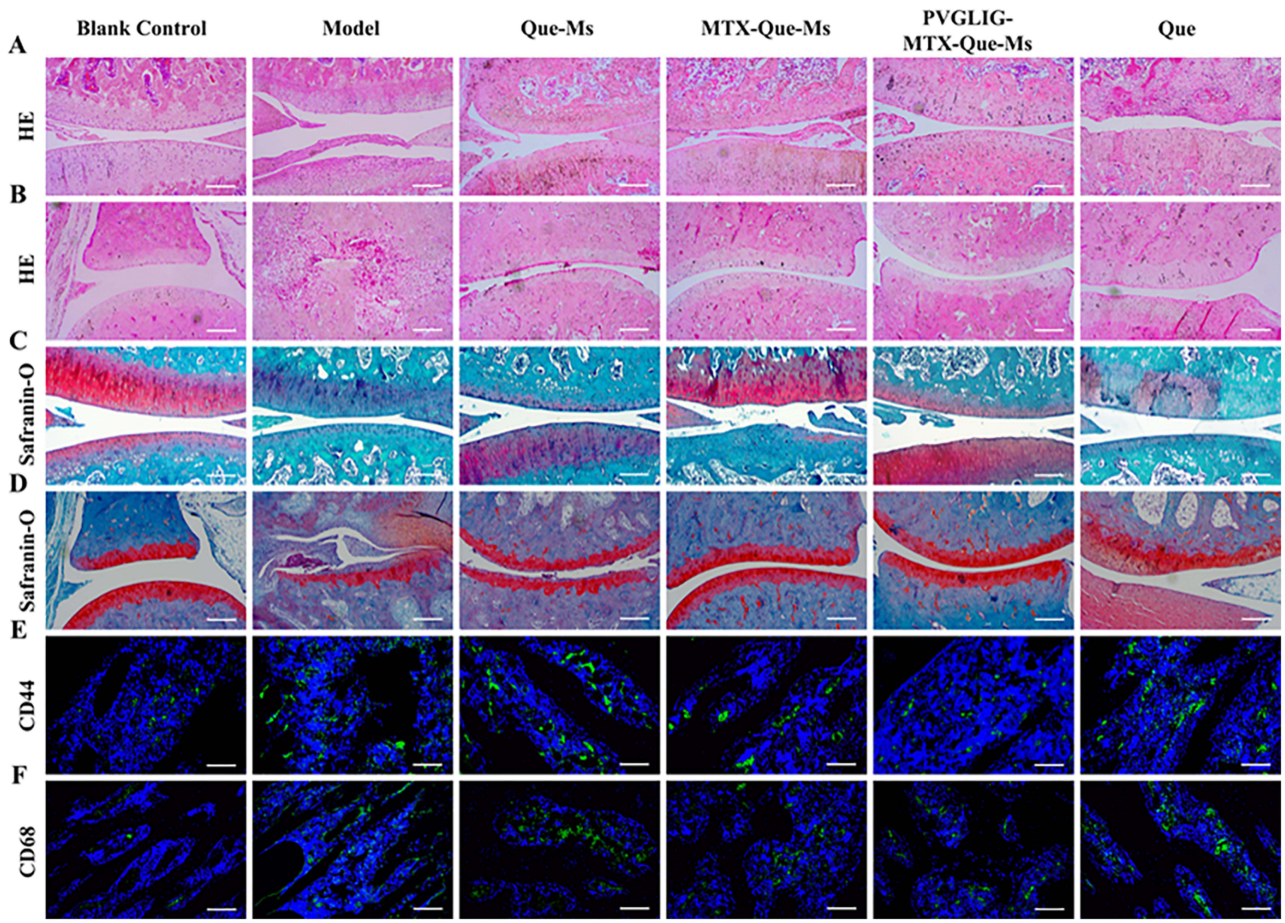

Figure 7 Histology analysis of cartilage sections in CIA rats. (**A**) HE staining of knee joint sections after treatment, scale bar, 100μm. (**B**) HE staining of ankle joint sections after treatment, scale bar, 100μm. (**C**) Safranin O staining of knee joint sections after treatment, scale bar, 100μm. (**D**) Safranin O staining of ankle joint sections after treatment, scale bar, 100μm. (**E** and **F**) Images of immunofluorescence results of CD44 and CD68 in cartilage sections after treatment, scale bar=50 μm. Data are presented as the mean SD (n=6).

RA patients. Therefore, this rat model is extensively used in RA-related studies.[29] To observe the real-time distribution of drug-carrying micelles in vivo, an in vivo imaging system was used to record and analyze the images. All drug-carrying micelles accumulated in large quantities in the joints of the rats, but PVGLIG-MTX-Que-Ms remained for a longer period in the joints. This suggested that PVGLIG-MTX-Que-Ms have good targeting abilities and exert slow-release effects. Compared with the control group, the model group demonstrated significantly higher joint swelling and large secretion of inflammatory factors. The drug-loaded micelles significantly reduced the joint swelling rate, lowered the arthritis scores of the CIA rats, inhibited the expression of inflammatory factors, and effectively controlled inflammation. During the joint histopathological examination, the PVGLIG-MTX-Que-Ms group exhibited a significant reduction in synovial inflammation and bone erosion compared with the model group, indicating that RA was successfully treated. CD44 and CD68 are overexpressed in the macrophages of RA patients.[30,31] Immunofluorescence results unveiled that CD44 and CD68 expression levels were significantly reduced in the cartilage of the treated CIA rats. According to the in vivo experiments, PVGLIG-MTX-Que-Ms played a good anti-inflammatory and chondroprotective effect by targeting the joints, inhibiting proinflammatory cytokines, and reducing the expression of inflammatory receptors. Moreover, no obvious histological damage or change was observed in major organs with PVGLIG-MTX-Que-Ms, and their safety was satisfactory.

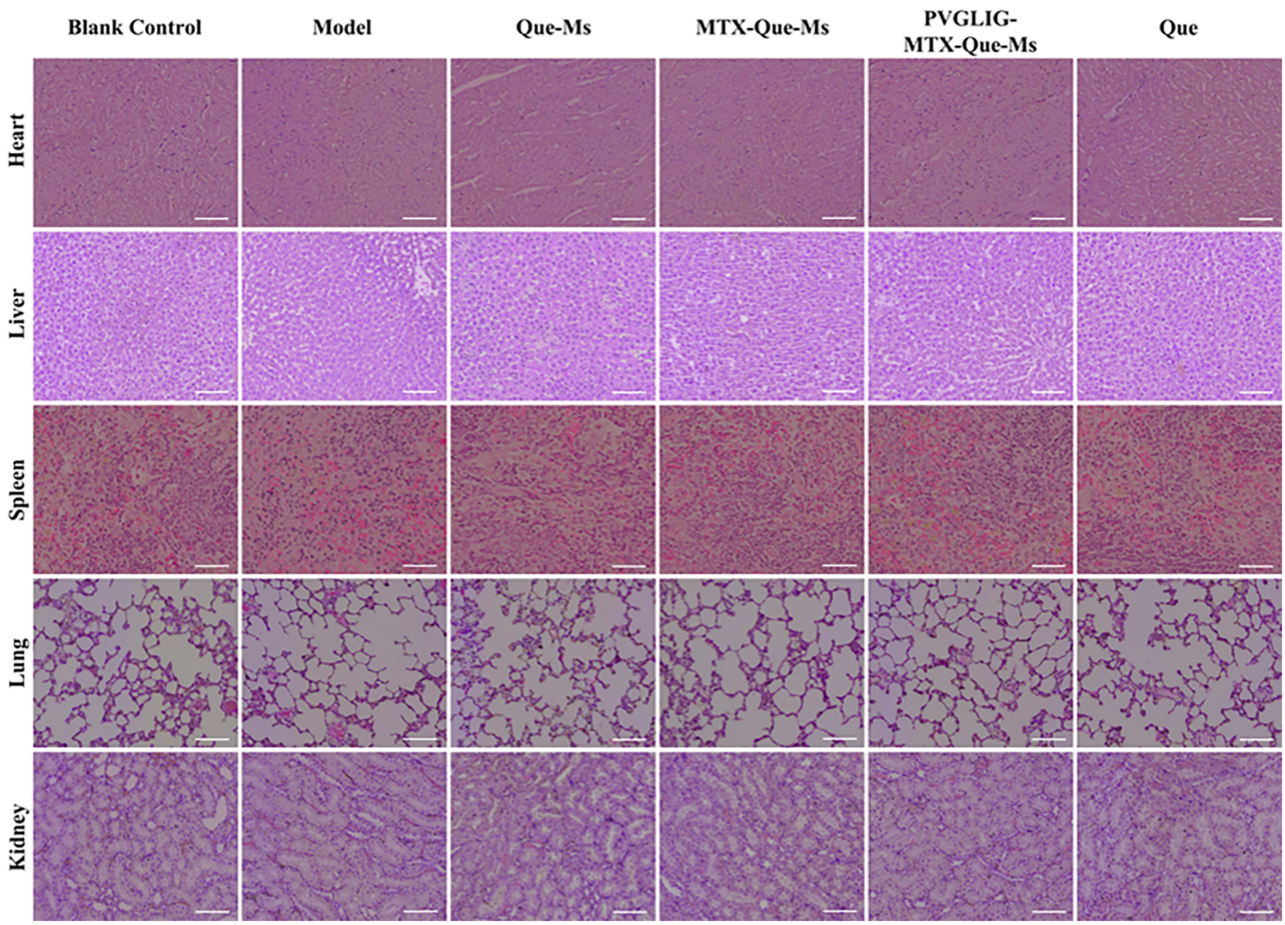

Figure 8 HE staining assay of major organs, scale bar=50 μm (n=6).

Conclusion

In summary, we successfully prepared a drug-carrying micelle with MMP2 enzyme sensitization based on MTX-targeted. PVGLIG-MTX-Que-Ms exhibited a small particle size a uniform distribution, and good biocompatibility and safety. It delayed drug release. According to in vitro studies, PVGLIG-MTX-Que-Ms utilized PVGLIG enzyme-sensitive peptides so that they accumulate at the inflammatory site, actively target activated macrophages, specifically release drugs, enhance the anti-inflammatory effect of drugs, and reduce the expression of inflammation-related markers. In vivo treatment and histological analysis revealed that PVGLIG-MTX-Que-Ms accumulated in the inflamed joints and were retained for a long time. PVGLIG-MTX-Que-Ms treatment significantly reduced cartilage damage and bone destruction in the CIA rats inhibited RA development, and provided a new direction for RA treatment.

Abbreviations

RA, rheumatoid arthritis; PVGLIG-MTX-Que-Ms, mmp enzymes respond to peptide and methotrexate modified quercetin micelles; CVD, chronic inflammation-induced cardiovascular disease; MMP, matrix metalloproteinases; Que, quercetin; PVGLIG, MMP-responsive peptide; MTX, methotrexate; Ms, micelles; FR-β, folate receptor-β; LPS, lipopolysaccharide; DiR, 1.1-dioctadecyl-3,3,3,3-tetramethylindotricarbocyanine iodide; SRB, Sulforhodamine B; Cou, coumarin.

Acknowledgments

Yandong Li is the principal corresponding author and Yingli Wang is the secondary correspongding author for this study. This work was supported by the National Natural Science Foundation of China (Grant No. 81903813), the Shanxi

Province Natural Science Foundation General Project (No. 202303021211171), the Scientific and Technological Innovation Ability Cultivation Project of Shanxi University of Chinese Medicine (Grant No. 2022PY-TH-12), the Scientific Research Fund of Shanxi Administration of Traditional Chinese Medicine (Grant No. 2022ZYYC087), and the Discipline Construct Funds of Shanxi University of Chinese Medicine (Grant No. 2023XKJS-26).

Disclosure

The authors report no conflicts of interest in this work.

References

1. McInnes IB, Schett G. Pathogenetic insights from the treatment of rheumatoid arthritis. *Lancet*. 2017;389(10086):2328–2337. doi:10.1016/S0140-6736(17)31472-1
2. Mateen S, Zafar A, Moin S, Khan AQ, Zubair S. Understanding the role of cytokines in the pathogenesis of rheumatoid arthritis. *Clin Chim Acta*. 2016;455:161–171. doi:10.1016/j.cca.2016.02.010
3. Smolen JS, Aletaha D, McInnes IB. Rheumatoid arthritis. *Lancet*. 2016;388(10055):2023–2038. doi:10.1016/S0140-6736(16)30173-8
4. Zhang L, Zhang Y, Pan J. Immunopathogenic mechanisms of rheumatoid arthritis and the use of anti-inflammatory drugs. *Intractable Rare Dis Res*. 2021;10(3):154–164. doi:10.5582/irdr.2021.01022
5. Tardito S, Martinelli G, Soldano S, et al. Macrophage M1/M2 polarization and rheumatoid arthritis: a systematic review. *Autoimmun Rev*. 2019;18(11):102397. doi:10.1016/j.autrev.2019.102397
6. Zheng X, Yu X, Wang C, et al. Targeted co-delivery biomimetic nanoparticles reverse macrophage polarization for enhanced rheumatoid arthritis therapy. *Drug Deliv*. 2022;29(1):1025–1037. doi:10.1080/10717544.2022.2057616
7. Boutet MA, Courties G, Nerviani A, et al. Novel insights into macrophage diversity in rheumatoid arthritis synovium. *Autoimmun Rev*. 2021;20(3):102758. doi:10.1016/j.autrev.2021.102758
8. Liu W, Zhang Y, Zhu W, et al. Sinomenine Inhibits the Progression of Rheumatoid Arthritis by Regulating the Secretion of Inflammatory Cytokines and Monocyte/Macrophage Subsets. *Front Immunol*. 2018;9:2228. doi:10.3389/fimmu.2018.02228
9. Goyal A, Agrawal N. Quercetin: a Potential Candidate for the Treatment of Arthritis. *Curr Mol Med*. 2022;22(4):325–335. doi:10.2174/1566524021666210315125330
10. Shen P, Lin W, Deng X, et al. Potential Implications of Quercetin in Autoimmune Diseases. *Front Immunol*. 2021;12:689044. doi:10.3389/fimmu.2021.689044
11. Kumazawa Y, Kawaguchi K, Takimoto H. Immunomodulating effects of flavonoids on acute and chronic inflammatory responses caused by tumor necrosis factor alpha. *Curr Pharm Des*. 2006;12(32):4271–4279. doi:10.2174/138161206778743565
12. Tang M, Zeng Y, Peng W, et al. Pharmacological Aspects of Natural Quercetin in Rheumatoid Arthritis. *Drug Des Devel Ther*. 2022;16:2043–2053. doi:10.2147/DDDT.S364759
13. Gokhale JP, Mahajan HS, Surana SJ. Quercetin loaded nanoemulsion-based gel for rheumatoid arthritis: *in vivo* and *in vitro* studies. *Biomed Pharmacother*. 2019;112:108622. doi:10.1016/j.biopha.2019.108622
14. Wang K, Yin C, Ye X, et al. A Metabolic Driven Bio-Responsive Hydrogel Loading Psoralen for Therapy of Rheumatoid Arthritis. *Small*. 2023;19(21):e2207319. doi:10.1002/smll.202207319
15. Canavan M, Marzaioli V, McGarry T, et al. Rheumatoid arthritis synovial microenvironment induces metabolic and functional adaptations in dendritic cells. *Clin Exp Immunol*. 2020;202(2):226–238. doi:10.1111/cei.13479
16. Nakashima-Matsushita N, Homma T, Yu S, et al. Selective expression of folate receptor beta and its possible role in methotrexate transport in synovial macrophages from patients with rheumatoid arthritis. *Arthritis Rheum*. 1999;42(8):1609–1616. doi:10.1002/1529-0131(199908)42:8
17. Nogueira E, Sárria MP, Azoia NG, et al. Internalization of Methotrexate Conjugates by Folate Receptor-α. *Biochemistry*. 2018;57(49):6780–6786. doi:10.1021/acs.biochem.8b00607
18. Angulo-Pachón CA, Pozo V, Miravet JF. Alkaline cations dramatically control molecular hydrogelation by an amino acid-derived anionic amphiphile. *J Colloid Interface Sci*. 2023;635:524–534. doi:10.1016/j.jcis.2022.12.134
19. Palsson-McDermott EM. Pyruvate kinase M2 regulates Hif-1α activity and IL-1β induction and is a critical determinant of the warburg effect in LPS-activated macrophages. *Cell Metab*. 2015;21(1):65–80. doi:10.1016/j.cmet.2014.12.005
20. Yao Q, Liu Y, Kou L, Tu Y, Tang X, Zhu L. Tumor-targeted drug delivery and sensitization by MMP2-responsive polymeric micelles. *Nanomedicine*. 2019;19:71–80. doi:10.1016/j.nano.2019.03.012
21. Dai Z, Tu Y, Zhu L. Multifunctional Micellar Nanocarriers for Tumor-Targeted Delivery of Hydrophobic Drugs. *J Biomed Nanotechnol*. 2016;12(6):1199–1210. doi:10.1166/jbn.2016.2249
22. Zhang X, Xu X, Chen J, et al. Identification of HHT-9041P1: a novel potent and selective JAK1 inhibitor in a rat model of rheumatoid arthritis. *Int Immunopharmacol*. 2023;125(Pt A):111086. doi:10.1016/j.intimp.2023.111086
23. Yu C, Liu H, Guo C, et al. Dextran sulfate-based MMP-2 enzyme-sensitive SR-A receptor targeting nanomicelles for the treatment of rheumatoid arthritis. *Drug Deliv*. 2022;29(1):454–465. doi:10.1080/10717544.2022.2032482
24. Guo RB, Zhang XY, Yan DK, et al. Folate-modified triptolide liposomes target activated macrophages for safe rheumatoid arthritis therapy. *Biomater Sci*. 2022;10(2):499–513. doi:10.1039/d1bm01520f
25. Zhu W, Song Z, Wei P, et al. Y-shaped biotin-conjugated poly (ethylene glycol)-poly (epsilon-caprolactone) copolymer for the targeted delivery of curcumin. *J Colloid Interface Sci*. 2015;443:1–7. doi:10.1016/j.jcis.2014.11.073
26. Liu Y, Xie B, Li L, et al. PEGylated lipid microspheres loaded with cabazitaxel for intravenous administration: stability, bioavailability, antitumor efficacy, and toxicity. *Drug Deliv Transl Res*. 2018;8(5):1365–1379. doi:10.1007/s13346-018-0562-0
27. Yang S, Zhao M, Jia S. Macrophage: key player in the pathogenesis of autoimmune diseases. *Front Immunol*. 2023;14:1080310. doi:10.3389/fimmu.2023.1080310

28. Song Y, Gao N, Yang Z, et al. Characteristics, polarization and targeted therapy of mononuclear macrophages in rheumatoid arthritis. *Am J Transl Res*. 2023;15(3):2109–2121.
29. Kong JS, Jeong GH, Yoo SA. The use of animal models in rheumatoid arthritis research. *J Yeungnam Med Sci*. 2023;40(1):23–29. doi:10.12701/jyms.2022.00773
30. Jia N, Gao Y, Li M, et al. Metabolic reprogramming of proinflammatory macrophages by target delivered roburic acid effectively ameliorates rheumatoid arthritis symptoms. *Signal Transduct Target Ther*. 2023;8(1):280. doi:10.1038/s41392-023-01499-0
31. Li Y, Liang Q, Zhou L, et al. An ROS-responsive artesunate prodrug nanosystem co-delivers dexamethasone for rheumatoid arthritis treatment through the HIF-1α/NF-κB cascade regulation of ROS scavenging and macrophage repolarization. *Acta Biomater*. 2022;152:406–424. doi:10.1016/j.actbio.2022.08.054